



**HAL**  
open science

# Frequency Domain Instantaneous Wavenumber Estimation for Damage Quantification in Layered Plate Structures

Olivier Mesnil, Hao Yan, Massimo Ruzzene, Kamran Paynabar, Jianjun Shi

► **To cite this version:**

Olivier Mesnil, Hao Yan, Massimo Ruzzene, Kamran Paynabar, Jianjun Shi. Frequency Domain Instantaneous Wavenumber Estimation for Damage Quantification in Layered Plate Structures. EW-SHM - 7th European Workshop on Structural Health Monitoring, IFFSTTAR, Inria, Université de Nantes, Jul 2014, Nantes, France. hal-01022998

**HAL Id: hal-01022998**

**<https://inria.hal.science/hal-01022998>**

Submitted on 11 Jul 2014

**HAL** is a multi-disciplinary open access archive for the deposit and dissemination of scientific research documents, whether they are published or not. The documents may come from teaching and research institutions in France or abroad, or from public or private research centers.

L'archive ouverte pluridisciplinaire **HAL**, est destinée au dépôt et à la diffusion de documents scientifiques de niveau recherche, publiés ou non, émanant des établissements d'enseignement et de recherche français ou étrangers, des laboratoires publics ou privés.

## FREQUENCY DOMAIN INSTANTANEOUS WAVENUMBER ESTIMATION FOR DAMAGE QUANTIFICATION IN LAYERED PLATE STRUCTURES

Olivier Mesnil<sup>1</sup>, Hao Yan<sup>2</sup>, Massimo Ruzzene<sup>1,3</sup>, Kamran Paynabar<sup>2</sup>, Jianjun Shi<sup>2</sup>

<sup>1</sup> D. Guggenheim School of Aerospace Engineering, Georgia Institute of Technology, Atlanta, GA, 30332, US

<sup>2</sup> H. Milton Stewart School of Industrial & Systems Engineering, Georgia Institute of Technology, Atlanta, GA, 30332, US

<sup>3</sup> G. W. Woodruff School of Mechanical Engineering, Georgia Institute of Technology, Atlanta, GA, 30332, US

Contact : omesnil3@gatech.edu

### ABSTRACT

Guided wavefield detection is at the basis of a number of promising techniques for the identification and the characterization of damage in plate structures. Among the processing techniques proposed, the estimation of instantaneous wavenumbers can be used as an effective metric that localize and quantifies delaminations in composite plates. A process able to estimate the in-plane and out-of-plane (depth) coordinate of a feature in a 2D structure using the Frequency Domain Instantaneous Wavenumber (FDIW) damage quantification technique is detailed in this paper. A post processing algorithm using a smooth sparse decomposition is used to highlight the studied features. The effectiveness of this method combined to the post processing technique is demonstrated for both numerical and experimental cases. This proposed methodology can be considered as a first step towards a hybrid structural health monitoring/ nondestructive evaluation (SHM/NDE) approach for damage assessment in composites.

**KEYWORDS :** *Structural Health Monitoring, Lamb Wave Propagation, Non Destructive Evaluation, Smooth Sparse Decomposition Algorithm*

### 1. INTRODUCTION

Guided wavefield detection is at the basis of a number of promising techniques for the identification and the characterization of damage in plate structures. With the continued and expanded use of composite materials in aerospace applications, techniques that can provide quantitative and detailed damage information are needed. Guided wave methods have long been investigated as a promising approach for structural health monitoring (SHM) applications in plate-like structures, and progress has been made in using guided waves to locate damage in composites [1, 2]. In SHM techniques, a small number of in-situ sensors are used to excite and receive guided waves. A proposed concept of hybrid SHM/nondestructive evaluation (NDE) is combining guided wave excitation via in-situ SHM sensors with scanning laser Doppler vibrometry to yield the detailed damage information that is required for prognostics (e.g., feeding detailed damage information into damage progression models for remaining life predictions). Advanced processing techniques can be applied to wavefield data in order to reveal damage information. Among the guided wavefield processing techniques proposed, the estimation of instantaneous and local wavenumbers can lead to effective metrics that quantify the extent of delamination damage in composite plates.

This paper illustrates the application of a frequency domain instantaneous wavenumber damage quantification technique for high frequency guided wave interrogation and of a smooth sparse decomposition algorithm to efficiently and automatically separate the defect region of any shape under the noise observation. The average effective depth of the selected defect area from the algorithm is

computed afterwards. The wavenumber technique is first described and applied to a simple numerical example in Section 2.1. The choice of the parameters for the analysis is then described in Section 2.2. The effectiveness of the technique for an experiment made with a simple damaged geometry is shown in Section 2.3. Finally the smooth sparse decomposition algorithm is developed in Section 3.

## 2. FREQUENCY DOMAIN INSTANTANEOUS WAVENUMBER

### 2.1 Concepts & Definitions

#### 2.1.1 The Instantaneous Wavenumber

For a recorded wavefield, the Instantaneous Wavenumber (IW) is a local function of the wavenumber at any instant of time. For a 1D problem, the IW is defined as the spatial derivative of the phase of the complex wavefield. In order to avoid phase unwrapping, the IW is computed by Equation 1 where  $g(x,t)$  is the Hilbert transform of the displacement function of the wavefield and  $k$  is its wavenumber. The mathematical process is fully described by Rogge and Parker [3].

$$k(x,t) = \text{imag} \left( \frac{\frac{\partial g(x,t)}{\partial x}}{g(x,t)} \right) \quad (1)$$

For a 2D case, the IW is given by  $IW(x,y,t) = \sqrt{k_x^2(x,y,t) + k_y^2(x,y,t)}$ .

In a general case, the IW is a function of the wavenumbers of all the excited modes. However, if only one mode is present at a given spatial point and time, the IW is a direct measure of the wavenumber of that mode. Moreover, if several modes are superimposed but one of them is dominant (higher amplitude and/or wavenumber), the IW is a measure of the wavenumber of the dominant mode only. This is, in general, the case when only the A0 (asymmetric) and the S0 (symmetric) modes are created due to an excitation, since the amplitude and the wavenumber of the A0 mode are higher than the S0 mode.

Figure 1b is the IW mapping for artificial data (Figure 1a) created using wavepackets of 5 and 11 rad/m. The IW directly measures the wavenumbers of the wavepackets since they are spatially separated.

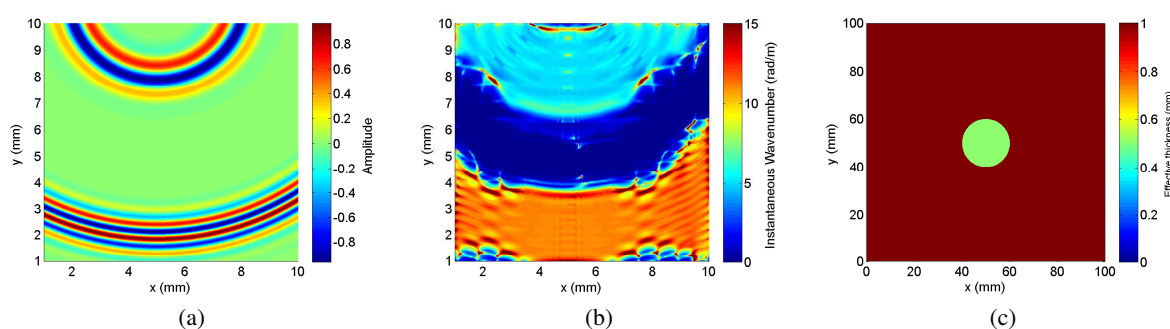


Figure 1 : (a): Artificial data with wavepackets of 5 and 11 rad/m, (b): IW map associated to the artificial data and (c): Theoretical Effective thickness of 1 mm thick plate with a mid-thickness circular delamination

#### 2.1.2 Effective Thickness

The Effective Thickness defines the subsurface depth of any features such as delaminations. For a pristine plate, the Effective Thickness is a constant equal to the thickness of the plate. For a plate

with a local subsurface feature, the Effective Thickness is a local value equal to the depth from the measurement surface to the feature at its location and equal to the thickness of the plate elsewhere. The theoretical Effective Thickness mapping of a square plate with a mid-thickness circular delamination at its center is shown in Figure 1c.

All the dispersion relations are computed using a Semi-Analytical Finite Element method (SAFE) detailed in [4]. The wavenumber is related to the Effective Thickness using dispersion relations (Figure 2a). For a layered plate, as the features are more likely to be found between the lamina, the Effective Thickness is a discrete quantity with  $N - 1$  possible values, where  $N$  is the number of lamina.

The variations of the wavenumber of the A0 and the S0 modes for an 8 ply composite glass fiber plate as a function of the Effective Thickness at 100 kHz are plotted in Figure 2b. It is important to note that the wavenumber of the A0 mode would increase over the delaminated area while the wavenumber of the S0 mode would decrease. However, since the A0 mode is dominant compared to the S0 mode, a local increase in the IW mapping is expected in the featured area.

The wavenumber vs frequency curve for the first four modes of the glass fiber composite plate which will be later used in the experiment is displayed in Figure 2c. The dispersion relations in the pristine part of the plate are the solid lines, while the dashed lines are the dispersion relations for the first three layers, which would correspond to an effective thickness of 3 (the unit here is the number of undamaged layer).

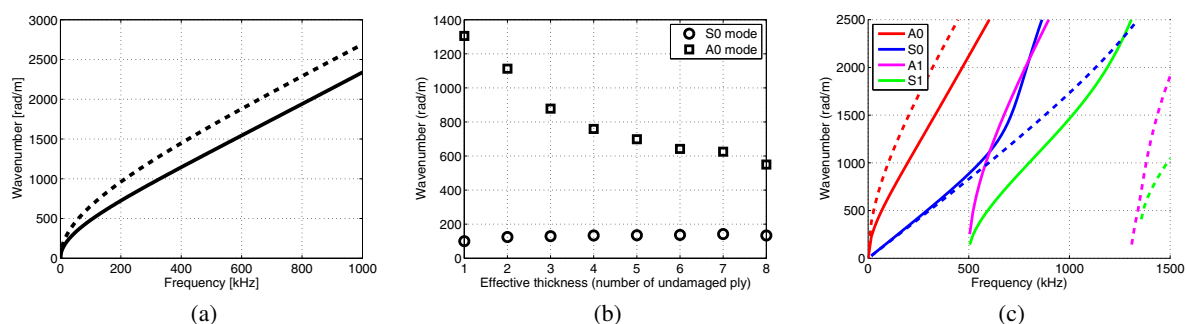


Figure 2 : (a): Dispersion relation of the A0 mode for a 1 mm thick (dashed line) and 2 mm thick (solid line) aluminium plate, (b): Wavenumber vs Effective Thickness curve for S0 (dashed line) and A0 (solid line) modes of an 1.6 mm thick glass fiber composite plate and (c) Wavenumber vs Frequency curve for the first four modes of a 8 ply 1.6 mm thick (solid line) and the first 3 ply (dashed line) of the same glass fiber composite plate

### 2.1.3 The Frequency Domain Instantaneous Wavenumber and Numerical Results

The IW is a very powerful tool used to compute a wavenumber map from a wavefield at a given instant of time. However since only a frequency and a wavenumber are needed to determine the local Effective Thickness, knowing the wavenumber at each instant of time is unnecessary. Therefore, the IW algorithm is used in the frequency domain. To calculate the IW in the frequency domain, a time Fourier transform is applied to the wavefield, then the dominant frequency is extracted by selecting the frequency with the highest displacement amplitudes (dominant response frequency). Eventually the IW is applied in this frequency-space domain. To illustrate this concept, a numerical simulation of a 200 mm x 200 mm x 1.6 mm glass fiber composite plate of layup  $[0/90/\pm 45]_s$ , containing a 25 mm diameter circular delamination between the second and third ply is implemented with a 80 kHz 4 cycles sine burst excitation. The out-of-plane displacement is recorded during a sufficiently long time to observe the first reflection on the edges of the plate. As both the S0 and A0 modes are excited, those modes are superimposed in the Frequency-Space domain. However, as the A0 mode is the dominant mode, the IW is a measure of the A0 wavenumber only. Therefore, only the Wavenumber vs

Effective Thickness curve for the A0 mode is used to convert the IW map into the Effective Thickness map. Figure 3a depicts the frequency-space domain representation of this wavefield at the dominant propagation frequency (80 kHz) and Figure 3b is the IW mapping associated with the previous picture. The irregular pattern in the frequency-space domain representation immediately highlights the circular feature and the significant increase in the IW mapping accurately provides the in plane coordinate of the subsurface feature. The whole IW map is converted into an Effective Thickness mapping (see Figure 4a) by looking for the best match between each individual value of the IW mapping and the dispersion relations. Discontinuities and irregularities in the IW map (Figure 4a) is due to numeric instability as Equation 1 is not defined for  $g$  goes to zero. The same discontinuities can be seen in the Effective Thickness map and will later be removed by post processing.

Besides the discontinuities, the estimated Effective Thickness map (Figure 4a) seems very similar to the theoretical values (Figure 4b), validating the process in this simple low-noise case.

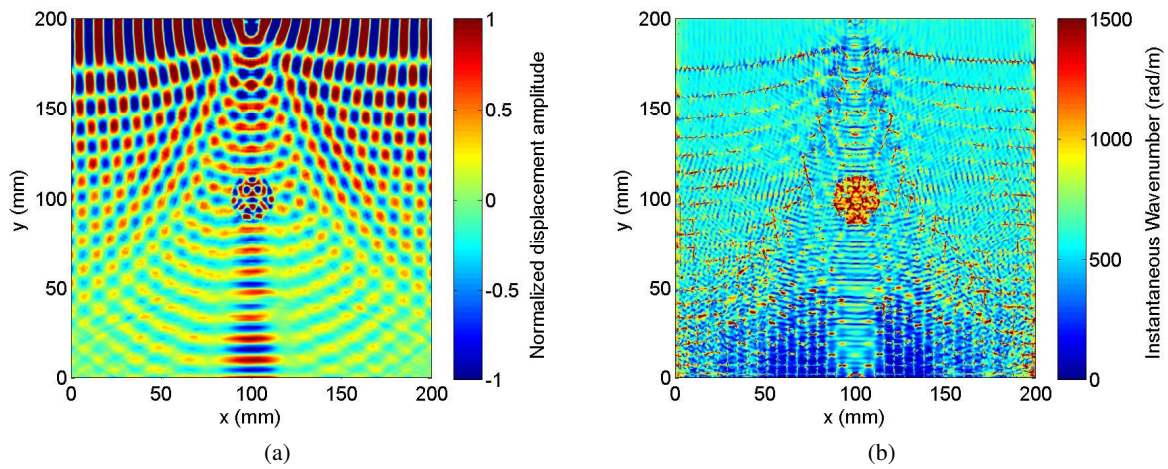


Figure 3 : (a): Frequency-Space domain at 80 kHz, (b): IW map associated to the Frequency Space domain representation

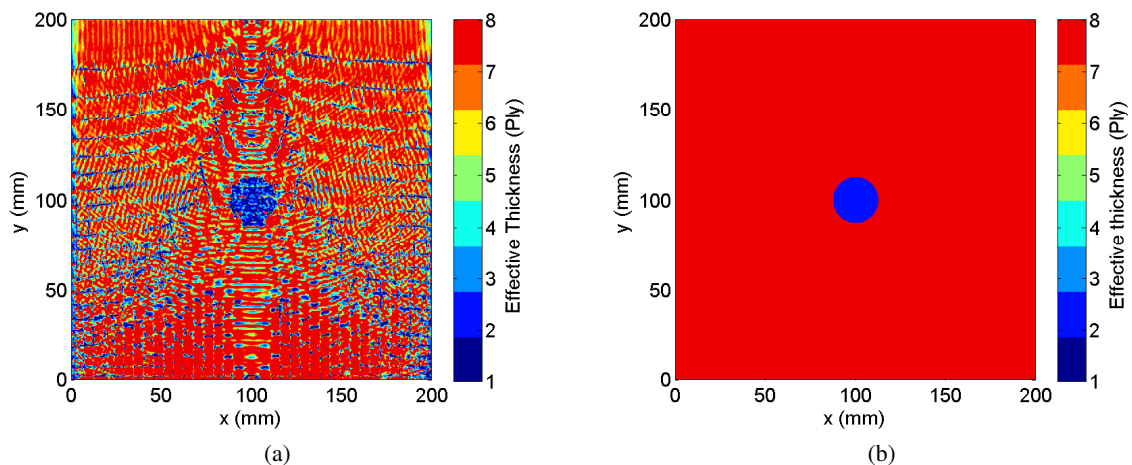


Figure 4 : (a): Effective Thickness map and (b): Theoretical Effective Thickness map

## 2.2 Choice of parameters

The choice of a many parameters during the wavefield acquisition (numerically generated or experimentally measured) is crucial. A poor choice can lead to misleading results. Among all the parameters, the most important are the following : The wavefield duration, the size of the spatial window of the recorded area, the spatial and time steps and the excitation (type and frequency).

The duration of the wavefield must be long enough to observe the propagation of all the excited modes through the scanned area. Typically the length of the recorded wavefield is equal to the time taken by the slowest excited mode to travel from the excitation source to the edges of the plate. The spatial window must include all the studied features. The main consequence of an overestimation of the spatial or time window is a dramatic increase of the data size and the computational time. However, and underestimation of those parameters would result in wrong or biased results.

The upper bound of the time and spatial steps is found using the Nyquist theorem. The calculation of the maximum spatial step requires the knowledge of the wavelengths of all the propagating modes and can be computed using SAFE [4]. Using too small time and/or spatial steps would also result into a substantial increase of the data size and computational time but correct results however if the time and/or spatial step is too big, the result given by the technique would be irrelevant.

To excite the structure at the desired frequency a 4 cycles sine burst is used. In order to simplify the data processing and avoid mode filtering, it is wise to select a frequency at which only the A0 and S0 modes propagate. For example given Figure 2c the excitation must be less than 500 kHz for this glass fiber composite plate. The choice of the excitation frequency must also be made considering the fact that the wavelength of the A0 mode propagating in the pristine plate must be at least twice smaller than the typical size of the damage.

## 2.3 Experimental Results

Experiments have been conducted in order to further study the Frequency Domain IW technique and to confirm its efficiency for a simple damage geometry. The experimental setup uses a 600 mm x 600 mm x 1.6 mm glass fiber S2 composite plate of layup  $[0/90/\pm 45]_s$  with an artificially created 25 mm diameter circular delamination between the 2<sup>nd</sup> and the 3<sup>rd</sup> ply manufactured at the Dipartimento di Ingegneria Aerospaziale of the Politecnico di Milano, Italy. The delamination is created by inserting a infinitesimally thin teflon disk between two layers to prevent the matrix to bond into a given area. The plate is excited by a piezo transducer located at 100 mm from the delaminated area. The out of plane velocity is recorded by a scanning vibrometer Polytec PSV-400 using the Doppler effect. The experimental setup is similar to the one used in reference [5]. In order to meet the requirements described in the previous section, the excitation is a 300 kHz 4 cycles sine burst. This excitation frequency does not excite the A1/S1 modes and provide a wavelength of 4.6mm in the pristine area (see Figure 2c), which is more than 5 times smaller than the typical size of the feature.

The scanned area is centered on the delamination region. Since the velocities of the S0 and A0 modes are very different at this frequency, they do not overlap in the scanned area. The wavefield is recorded until the A0 mode reaches the edges of the plate. Figures 5 show the interaction of the S0 and the A0 modes with the delaminated area. The amplitude of the A0 mode is about 100 times greater than the one of the S0 mode and its wavenumber is about 5 times larger, therefore the Frequency-Space representation is dominated by the A0 mode and the IW is a measure of the Wavenumber of the A0 mode.

The dominant frequency of the experimentally recorded wavefield is 300 kHz. The frequency-space representation of the wavefield is shown in Figure 5c and its associated IW mapping in Figure 6a

As the feature is hardly distinguishable in the frequency-space representation, the IW mapping clearly highlights the shape of the delaminated area. Using the dispersion relations of the studied plate,



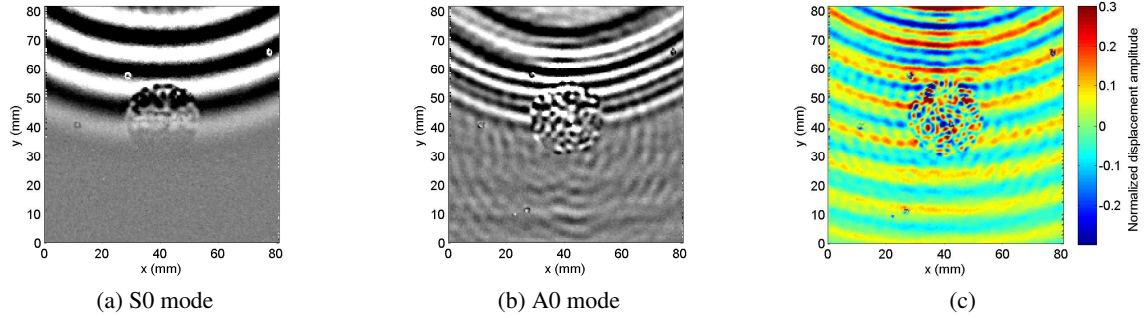


Figure 5 : (a) and (b): Interaction of the S0 ( $t = 40\mu s$ ) and A0 ( $t = 73\mu s$ ) modes with the delamination and (c): Frequency-Space domain

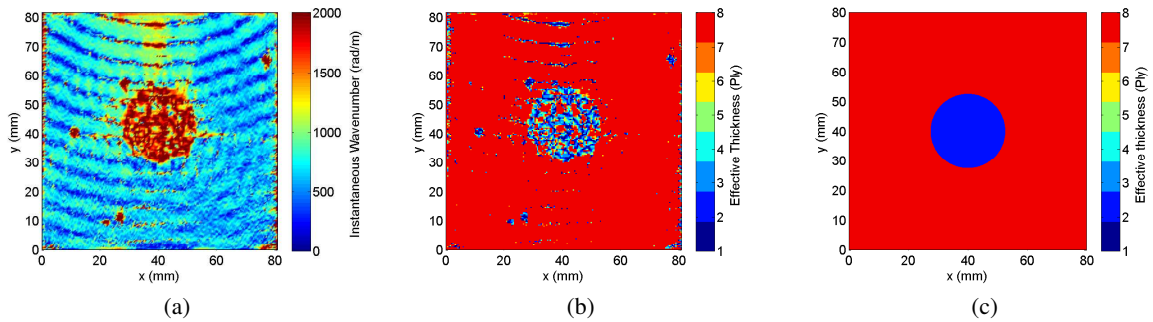


Figure 6 : (a): IW map, (b): Effective Thickness map and (c): Theoretical Effective Thickness map

the Effective Thickness map (Figure 6b) is created from the IW map. The theoretical Effective Thickness map is represented in Figure 6c. In this case, the frequency domain instantaneous wavenumber provides a correct estimation of the in plane size of the feature and its out-of-plane coordinate (depth). The same discontinuity issue than in the numerically simulated case is present and must be treated by additional post processing. The four smaller circular dots visible on Figure 6a and 6b are actually air bubbles underneath the scanning tape (needed to reflect the laser beam of the laser vibrometer) and are clearly visible on the sample.

### 3. POST PROCESSING TECHNIQUES

In this section, we develop a post-processing technique, which can achieve fast and automatic defect detection for guided wave-field experiments. We use the Smooth-Sparse decomposition algorithm [6] to detect and separate the delamination region from the IW map obtained in the previous section. The idea of Smooth-Sparse decomposition is to decompose the original noisy image  $Y$  to several components including the smooth background ( $Y_B$ ), the delaminated part ( $S$ ), and noises ( $E$ ). We further represent the background and defects (delaminations) using smooth basis (e.g., spline basis) of the functional space denoted by  $B$  and  $B_S$ , respectively. Consequently, the Smooth-Sparse decomposition model can be rewritten as  $Y = B\theta + B_S\theta_S + E$ , where  $\theta$  and  $\theta_S$  are the basis coefficients corresponding to  $Y_B$  and  $S$ , respectively. In addition, we assumed that the representation of the defect in the basis  $B_S$  is sparse. This assumption follows the recent development of compressive sensing, which reveals the fact that many natural signals and images are sparse or compressible in the sense that they have concise representation when expressed in the proper basis. Under these assumptions, this separation problem can be formalized as a penalized least square problem in Equation (2).

$$\underset{\theta, \theta_S}{\operatorname{argmin}} \|e\|^2 + \lambda \theta' R \theta + \gamma |\theta_S|_1 \quad \text{s.t.} \quad Y = B\theta + B_S \theta_S + E \quad (2)$$

Where  $R$  is the roughness matrix, and  $\lambda$  and  $\gamma$  are tuning parameters. The  $L_2$  penalty term  $\lambda \theta' R \theta$  regularizes the level of the mean smoothness, while the  $L_1$  penalty term  $\gamma |\theta_S|_1$  encourages the sparsity of defects. Since the formulation is convex, the global optimum can be achieved using block coordinate descent algorithm which is very efficient in the high dimensional settings. More details about the formulation and optimization algorithm is given in [6].

In both numerical and experimental studies, we use  $3 \times 3$  spline basis  $B$  for background, and  $40 \times 40$  spline basis  $B_S$  for the defect part. As the guided wave can only detect the defect size larger than one-half the wavelength, the number of basis should be large enough to capture the window size of one-half the wavelength.

We apply the Smooth-Sparse decomposition to analyse the thickness map obtained from the numerical study. The effective thickness of the delaminated region detected by the smooth-sparse decomposition is shown in Figure 7a to be compared with the true feature shown in 4b, respectively. The performance of the decomposition method is evaluated by comparing the detected delaminated region with the true region in terms of the false positive rate (FPR) and the false negative rate (FNR). The FPR refers to the percentage of pixels that are wrongly classified as defects. The FNR refers to the percentage of pixels not detected by the algorithm. We achieve the FPR as 0.3% and the FNR rate as 1.1%. The computation time is 0.26s using a 2.3Ghz CPU. The average effective thickness of the selected area is also 2.3, which is close to the actual depth between the 2<sup>nd</sup> and 3<sup>rd</sup> layers.

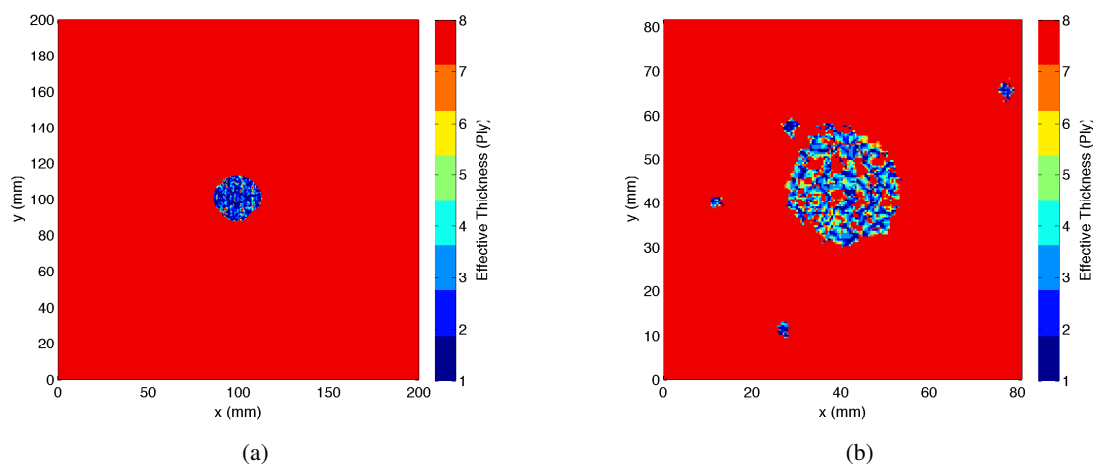


Figure 7 : (a): Effective thickness map after post processing for the numerical case, to be compared with Figure 4b (b) Effective thickness map after post processing for the experimental case, to be compared with Figure 6c

The same technique is applied to the experimental study, and the corresponding results are shown in Figure 7b. The ideal defect is a 25 mm diameter circular delamination as shown in Figure 6c. For this experiment, the FPR and FNR of the decomposition algorithm respectively are 3.54% and 4.66% and the computational time is 0.1475s. The larger values of FPR and FNR are because of several air bubbles introduced into the process, during the experiment. As can be seen in Figure 7b, the Smooth-Sparse algorithm detects both the circular defect and the four air bubbles around the defect, which increases the FPR and FNR values. The mean effective depth of the damaged area is around 4.20, which is greater than the actual depth between 2<sup>nd</sup> and 3<sup>rd</sup> layer. By computing the median of the effective thickness, this bias can be reduced. The median effective thickness in this case is 3. The



experimental noise, the presence of the air bubbles and the fact that both sides of the delamination are in contact with each other explain the overestimation of the average effective thickness compared to the ideal, non contact, low noise case (numerical simulation).

#### 4. CONCLUSION

A technique able to locate and quantify subsurface features in composite plates using a frequency domain instantaneous wavenumber has been developed. This technique has been applied on a simple damaged geometry as example for both numerical and experimental cases. In order to quickly and automatically interpret the output data of this technique, a smooth-sparse decomposition algorithm is used. The combination of those two techniques provides an accurate estimation of the size of the feature in both cases. The out of plane location of the feature is correct in the numerical case but overestimated in the experimental case. This overestimation is due to the fact that the delamination has been modelled as a void in the finite element software while the actual feature in the real life sample used in the experiment is created with a teflon disk, allowing contact between the upper and lower side of the feature. The total computational time for the numerical case is 0.46s using a 2.3 GHz computer (44% wavenumber technique and 56% post processing) for a final result made of 800\*800 pixels and the total computational time for the experimental case is 0.23s (40% wavenumber technique and 60% post processing) for a final result of 185\*193 pixels. As a future work, we are willing to study more complex damage geometries.

#### 5. ACKNOWLEDGEMENT

The work is funded by a collaborative agreement (*NRANNH11ZEA001N – VSST1*) between NASA LaRC and Georgia Tech and the Strategic University Partnership between Boeing and Georgia Tech.

#### 6. REFERENCES

- [1] H Sohn, D Dutta, JY Yang, HJ Park, MP DeSimio, and ED Swenson. Delamination detection in composites through guided wave field processing. *Composites Science and Technology*, 71:1250–1256, 2011.
- [2] David Barnoncel, Wieslaw J. Staszewski, Jochen Schell, and Patrick Peres. Damage detection in reusable launch vehicle components using guided ultrasonic waves and 3d laser vibrometry. *Proc. SPIE* 8695, page 86950D, 2013.
- [3] Matthew Rogge and Raymond Parker. Instantaneous wavenumber estimation of guided wavefield images for characterization of damage in composite structures. *NASA TM*, 2013.
- [4] Ivan Bartoli, Alessandro Marzani, Francesco Lanza di Scalea, and Erasmo Viola. Modeling wave propagation in damped waveguides of arbitrary cross-section. *Journal of Sound and Vibration*, 295(3):685–707, 2006.
- [5] Matteo Carrara and Massimo Ruzzene. Numerical and experimental analysis of guided waves propagation in composite plates. pages 86950W–86950W, 2013.
- [6] Hao Yan, Kamran Paynabar, and Jianjun Shi. Image defect detection with smooth-sparse decomposition. 2014.